THE BALTIC JOURNAL
OF ROAD AND BRIDGE ENGINEERING
2025/20(2)

ISSN 1822-427X/eISSN 1822-4288
2025 Volume 20 Issue 2: 1–23
https://doi.org/10.7250/bjrbe.2025-20.657

INTELLIGENT PREDICTION OF THE HORIZONTAL DEFORMATION DURING THE EXCAVATION PROCESS BASED ON PARTICLE SWARM OPTIMISATION AND SUPPORT VECTOR MACHINE

YU ZHANG[1,2], CHEN ZHANG[1,2], ZHIDUO ZHU[1,2]*, LIU YANG[1,2], HAO TANG[1,2]

[1]*School of Transportation, Southeast University, Nanjing, Jiangsu Province 211189, China*

[2]*Jiangsu Key Laboratory of Low Carbon and Sustainable Geotechnical Engineering, Jiangsu Province 211189, China*

Received 23 September 2024; accepted 26 May 2025

Abstract. The reasonable selection of soil layer parameters relates to the accurate prediction of the horizontal deformation of the foundation pit, which is the main problem of highway tunnel pit design. The aim of this paper is to obtain suitable soil layer parameters for finite element simulation of highway tunnel based on the particle swarm optimisation (PSO) and support vector machine (SVM). First, considering the overfitting problem of SVM in the inversion of soil parameters, the PSO was used to improve the SVM model. Second, the PSO-SVM model was trained with 25 groups of elastic modulus as input values and deformation as output values. Then, according to the monitored deformation data, the soil parameters were inverted by PSO-SVM model. Finally, the inversion parameters were substituted into the finite element model to predict the horizontal deformation of the foundation pit. The results showed that based on the inversion parameters of PSO-SVM model, the finite element method had a good accuracy in predicting the horizontal deformation of the foundation pit. The average relative error between the predicted value and monitored value was 2.95%.

* Corresponding author. E-mail: zzd13605192579@163.com

Therefore, the application of the parameter inversion method based on PSO-SVM had a reference value for tunnel pit design.

Keywords: deformation prediction, finite element simulation, highway tunnel pit, particle swarm optimisation, support vector machine.

Introduction

With the development of the economy, tunnel pit engineering is developing rapidly in China. The construction of tunnel pit engineering will inevitably cause deformation. When the deformation exceeds the safety limit, the safety work of tunnel pit engineering can be affected, resulting in adverse social impacts and endangering the safety of people (Zheng et al., 2016; Zhou et al., 2017). In order to ensure the safety of tunnel pit engineering, deformation prediction has become a hot topic in the engineering field (Shen et al., 2019).

Currently, there are two main methods for deformation prediction caused by tunnel pit construction. The first method is to use models such as long- and short-term memory network (LSTM) (Li et al., 2022), random forest (RF) (Feng et al., 2022; Xu et al., 2024), artificial neural network (ANN) (Liu et al., 2021; Guo et al., 2020; Liu et al., 2014), etc. These models are trained by using existing deformation monitoring data to predict the results, which require a large amount of monitoring data. The second method is to use finite element method (FEM) to simulate the construction process for obtaining the deformation value. The calculation results of FEM rely heavily on the selection of soil layer parameters. Some relevant research indicated that using static soil parameters to calculate the dynamic deformation of tunnel pit cannot get the optimal results (Ma et al., 2023; Amini & Ardestani, 2019). To solve these problems, more and more scholars integrate the monitoring data, physical and mechanical test results and machine learning algorithms. First, the construction process is simulated by finite element method. Then, the soil layer parameters are obtained by inversion method. Finally, the inverted parameters are used for simulation calculation to predict the deformation of subsequent construction. This technology has shown its superiority in many projects, providing a scientific basis for the safe design and construction of engineering design.

In the early 1970s, people began to determine various soil layer parameters from deformation measurement information (Wang et al., 1998). Most of the traditional inverse analysis methods were based on numerical methods (Kavanagh & Clough, 1971; Kirsten, 1976; Gioda & Maier, 1981). By optimising and modifying the parameters, the difference between the numerical results and monitored values was minimized. The method had a great range of application at that time. However, it was very difficult to establish a function to express the relationship between soil layer parameters and deformation (Sha & Chen, 2017). Facing the problems of the

traditional inverse analysis method, classical machine learning algorithms, such as BP neural network (Wang et al., 2007; Zhang et al, 2013; Xiao et al., 2017), GA-BP neural network (Gao et al., 2020; Jiang, 2013), PSO-BP neural network (Ling et al., 2020; Li et al., 2024), and other improved neural networks (Li & Sima, 2021; Zhao et al., 2023) were applied to the parameter inversion work. Unfortunately, the neural network was easy to fall into local optimisation, which cannot meet the accuracy requirements of parameter inversion. Compared with the models mentioned above, some scholars have proposed that SVM model has better advantages, such as more excellent generalization performance and faster convergence speed. However, in practical application it is required to pay attention to the reasonable value of parameters. Some studies showed that using PSO to optimise SVM parameter selection was helpful to the accuracy of soil layer parameter inversion (Ruan et al., 2021; Cheng et al., 2022; Jiang et al., 2011; Zhou et al., 2022; Chen et al., 2015]. However, most studies focused on statistical analysis of existing data. Few people considered the application of PSO-SVM combined with the finite element method to the deformation prediction of tunnel pit.

In order to obtain suitable soil layer parameters for finite element simulation of highway tunnel, this paper used PSO-SVM as an inversion tool. Based on the monitored data of the project, the soil layer parameters affected by excavation during the construction period of the tunnel were inverted. Then, the inverted parameters were input into the finite element model. The calculated deformation values were compared with the monitored values, and the pit deformation for the next excavation condition was predicted. The use of PSO-SVM in the inverse analysis method could make up for the shortcomings of the traditional parameter acquisition method. It also provided an effective method for selecting parameters of numerical simulation of tunnel pit.

1. Methodology

1.1. Support vector machines

Facing the problems of large computation and low generalization performance, scholars have turned their attention to the SVM model. SVM is a machine learning model based on the statistical learning theory and the principle of structural risk minimization. It is mainly used for classification and regression analysis (Ruan et al., 2019). The basic idea is to map the unclassifiable low-dimensional samples to a high-dimensional feature space. An optimal hyperplane is constructed in the high-dimensional space, which maximizes the distance from the sample point closest to the hyperplane (see Figure 1).

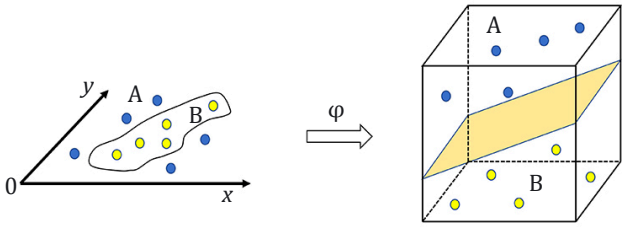

Figure 1. Mapping of indivisible low dimensions to divisible high dimensions

From the structural risk minimization principle, the objective function and the constraints for solving the support vector machine principle are shown in the following equation:

$$\min \varphi(\omega,b)=\frac{1}{2}\|\omega\|^2+C\sum_{i=1}^{n}\xi_i, \tag{1}$$

$$\text{s.t.} \quad y_i\left(\omega\cdot \boldsymbol{x}_i-b\right)\geq 1-\xi_i, \tag{2}$$

where ω is the weight vector; b is the bias term; ξ_i is the slack variable; C is the penalty parameter; y_i is the sample label; $\boldsymbol{x_i}$ is the feature vector.

This is a constrained optimisation problem, which is transformed into an unconstrained form using the Lagrange multiplier method:

$$\mathrm{L}(a,\omega,b)=\frac{1}{2}\|\omega\|^2+C\sum_{i=1}^{n}\xi_i-\sum_{i=1}^{n}a_i\left[y_i\left(\omega\cdot \boldsymbol{x_i}+b\right)-1+\xi_i\right]. \tag{3}$$

Finding its saddle point and transforming the problem:

$$\max \varphi(a)=\sum_{i=1}^{n}a_i-\frac{1}{2}\sum_{i,j=1}^{n}a_i a_j y_i y_j\langle\varphi\left(\boldsymbol{x_i}\right)\cdot\varphi\left(\boldsymbol{x_j}\right)\rangle; \tag{4}$$

$$\text{s.t.} \quad \sum_{i=1}^{n}a_i y_i=0; \tag{5}$$

$$0\leq a_i\leq C; i=1,2,...,n. \tag{6}$$

Using the KKT condition to solve, the final partition is obtained as follows:

$$F(x)=\operatorname{sgn}\sum_{Support\ Vector}a_i^0 y_i\langle\varphi\left(\boldsymbol{x_i}\right)\cdot\varphi\left(\boldsymbol{x_j}\right)\rangle-b_0. \tag{7}$$

The entire solution process only involves the inner product of two vectors and does not require the specific analytic form of the vectors in the feature space.

Therefore, it is only necessary to define the function $K(\boldsymbol{x_i}, \boldsymbol{x_j})$ such that for the mapping φ from the original space to the feature space it satisfies:

$$K\left(\boldsymbol{x_i}, \boldsymbol{x_j}\right) = \langle \varphi\left(\boldsymbol{x_i}\right) \cdot \varphi\left(\boldsymbol{x_j}\right) \rangle. \tag{8}$$

It is possible to solve the classification problem for nonlinear samples, and K is the kernel function.

1.2. Particle swarm optimisation

The reasonable value of the parameters of the support vector machine is the key to realising the function of the support vector machine. Due to these limitations, including low efficiency, scholars have proposed numerous swarm intelligence algorithms to optimise the value method. As one of the classical swarm intelligence algorithms, particle swarm optimisation (PSO) is mainly used in function optimisation, machine learning, fuzzy system control, and other research fields (Yang & Li, 2004). It can improve the performance of SVM by using PSO to solve the parameter value problem (Li et al., 2018). To realize the PSO, we assign initial random positions and initial random velocities to all particles. Then, the position of each particle will be updated according to the velocity of each particle, the known global optimal position, and the known optimal position. As the computation progresses, by exploring and utilising the known vantage points in the search space, the particles cluster around the optimal point. Each particle updates its velocity and position according to the following equation (see Figure 2).

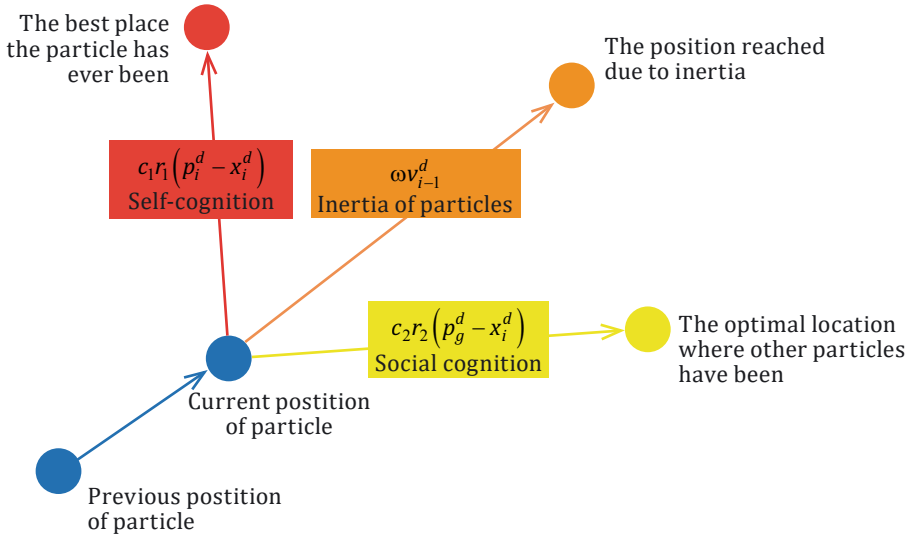

Figure 2. Particle update in PSO

$$v_i^d = \omega v_{i-1}^d + c_1 r_1 \left(p_i^d - x_i^d \right) + c_2 r_2 \left(p_g^d - x_i^d \right), \tag{9}$$

$$x_i^d = x_{i-1}^d + v_i^d, \tag{10}$$

where v_i^d is the velocity of the particle; x_i^d is the position of the particle; i = 1,2,...,m; d = 1,2,...,q; m is the number of particles; q is the dimension of the solution vector; w is the inertia weight; c_1, c_2 are the learning factors, c_1 represents the particle self-cognition, c_2 represents the particle social cognition, generally taking the value c_1 = c_2 = 2; r_1, r_2 are random numbers in [0,1].

1.3. Finite element method

Qingshan Tunnel project is located in Jiangsu Province, China. The total length of the tunnel is 1778 m. During the construction, the tunnel was divided into multiple construction sections according to different geological conditions. Each construction section adopted the most suitable excavation strategy and support measures. Some sections were even excavated more than 12 metres, which was a typical long tunnel deep foundation project.

In order to predict the deformation of tunnel pit, according to the example of Qingshan Tunnel project, the 3D finite element model of pit excavation was established using ABAQUS software. Considering the influence of the model size on the simulation results, the length, width and height of the model were set as follows:

(1) X-Direction: the left and right lines of the tunnel were extended to 100 metres on each side;
(2) Y-Direction: considering the continuity of support and the influence range of tunnel pit excavation, the extension of each side was determined to be 3.5 H (H is the excavation depth of tunnel pit). Thus, the starting mileage is K24 + 866 and the ending mileage is K24 + 954;
(3) Z-Direction: 100 m downward from the surface.

The size of 3D finite element model for tunnel pit was X × Y × Z = 200 × 88 × 100 m. The modelling part of the pit was shown in the red box, such as Figure 3.

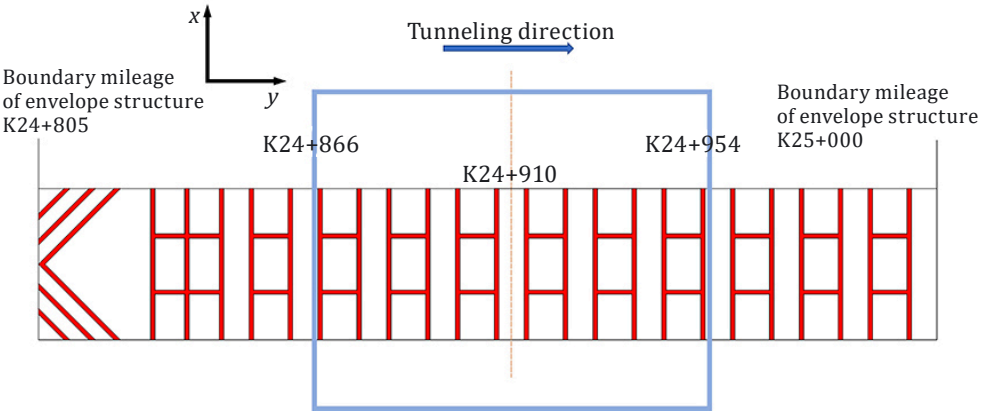

Figure 3. Top view of the simulated soil range

In this paper, the Mohr Coulomb model was chosen as the principal model. According to the ground investigation data, there were six soil (rock) layers distributed in the site, which are ①-2 topsoil layer, ③-1 silty clay layer, ③-2 silty clay layer, ③-3 silty clay layer, ⑤-1 round stone layer, and fully weathered and strongly weathered rock layer. Considering that the strongly weathered rock layer has a large depth and has little influence on the simulation results, so it is combined with the fully weathered rock layer in the modelling. It is possible to reduce the calculation amount of numerical simulation. The physical and mechanical parameters of each soil (rock) layer are shown in Table 1. The linear elastic model is used for the ground wall and support in the simulation process. The material property parameters are determined by the relevant standards and numerical simulation experience. The values of each material parameter are shown in Table 2.

Table 1. Values of physical-mechanical parameters of soil (rock)

Soil layer number and name	Thickness, m	Weight of soil, kN/m^3	Poisson's ratio	Cohesion, kPa	Angle of internal friction, °	Modulus of compression, MPa
①-2 Topsoil	0.7	18.8	0.39	10	8.8	5.70
③-1 Silty clay	2.8	19.3	0.37	24	15.0	7.92
③-2 Silty clay	5.3	19.4	0.38	22	18.0	6.68
③-3 Silty clay	13.2	19.2	0.37	22	18.0	11.37
⑤-1 Round stone	2.0	20.0	0.28	0	33.0	45
Fully weathered, strongly weathered rock	>20	23.4	0.25	200	32.0	1000

Two supports were arranged in the tunnel pit from top to bottom. The first one was 800 × 800 mm concrete support with a spacing of 8 m. The shape of the support was H-shaped. The second support was φ 609 steel pipe support with a wall thickness of 16 mm. The supporting structure and soil layer distribution at *K*24 + 910 are shown in Figure 4. According to the setting of supporting structure, the tunnel pit was excavated three times. The excavation depth was 2.2 m, 8 m, 12.5 m. The completed support structure and the three-dimensional tunnel pit model are shown in Figures 5 and 6.

Table 2. Parameter values of ground-connected wall and supporting structure

Type of structure	Density, kg/m^3	Modulus of elasticity, GPa	Poisson's ratio
Underground Diaphragm Wall	2400	30	0.2
Concrete Support	2400	30	0.2
Steel Support	7850	210	0.3

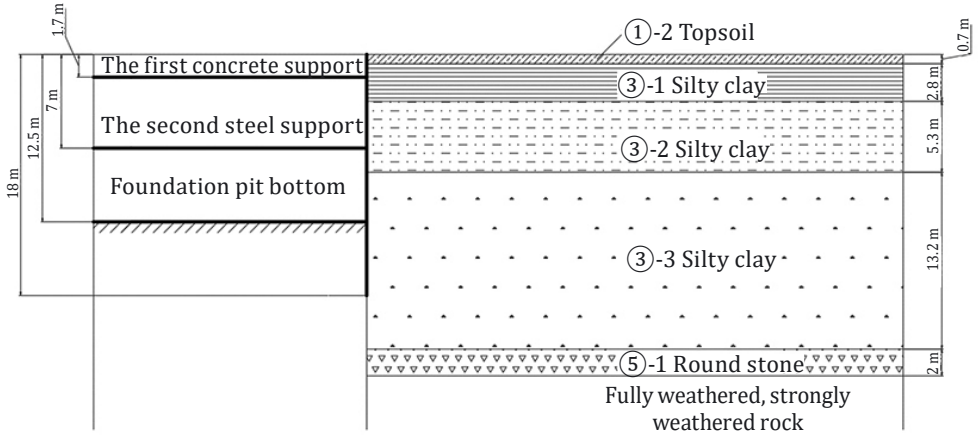

Figure 4. Support structure and soil layer distribution at K24+910

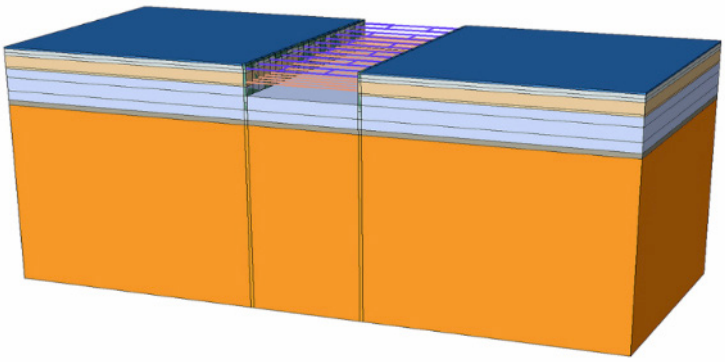

Figure 5. Finite element model of pit

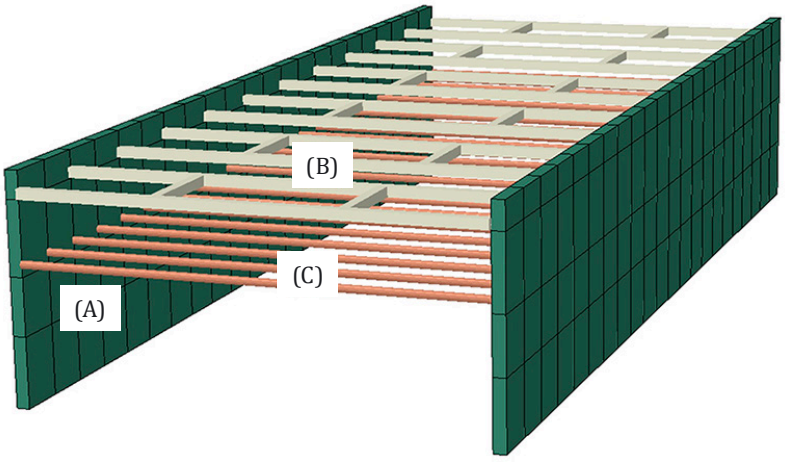

(A) – the model of underground diaphragm wall;
(B) – the model of the first concrete supports;
(C) – the model of the second steel supports.

Figure 6. Finite element model of enclosure and support structure

1.4. Inversion analysis process

Relying on the Yilu Expressway Qingshan Tunnel project, this paper used PSO to optimise SVM to invert the elastic modulus of the soil layer. Then, the inverted elastic modulus was substituted into the finite element model for numerical simulation analysis. The calculated results showed that the inverse analysis

parameters were reasonable. Furthermore, the horizontal deformation of the foundation pit in the next working condition was predicted. The specific inverse analysis process showed the following:

(1) Construction of training samples. According to the engineering experience and relevant literature, we used the soil compression modulus to determine the range of soil layer elastic modulus. The orthogonal test was carried out at the appropriate level to form multiple parameter combinations. These parameters were input into the finite element model to calculate the deformation data and form the training samples.
(2) Optimisation of algorithm parameters. PSO was used to optimise the penalty parameters and kernel parameters of SVM. Then, the optimal model parameters were obtained.
(3) Inversion of elastic modulus. The optimal model parameters obtained in the previous step were input into the Support Vector Machine. The soil layer elastic modulus was inverted using the deformation data from field monitoring. The inversion results were input into the finite element model to obtain the deformation. Then, the simulated deformation was compared with the monitoring data to verify the accuracy of the elastic modulus inversion.
(4) Prediction of pit deformation. Using the elastic modulus obtained from the inversion, the deformation at the end of the next excavation was simulated and predicted.

The flow chart of parameter inversion and deformation prediction in this paper is shown in Figure 7.

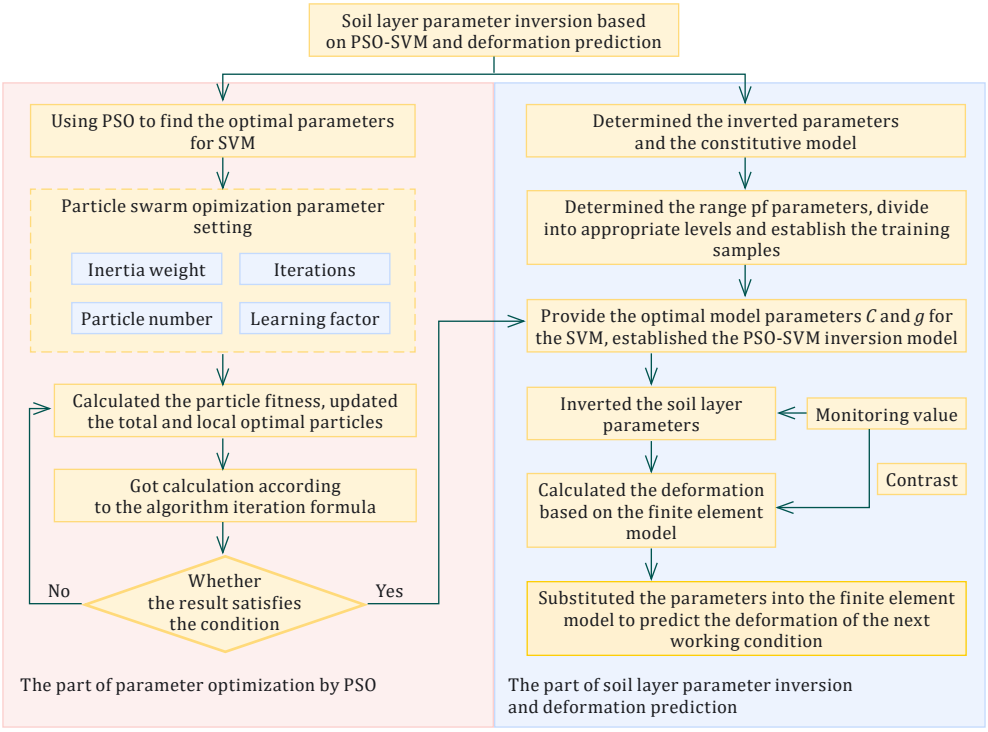

Figure 7. The flow chart of parameter inversion and deformation prediction

2. Results and discussion

2.1. Simulation results and deformation characterisation of tunnel pit

According to the investigation report, the relationship between the compression modulus and the elasticity modulus is shown in Table 3. Based on the current deep tunnel pit excavation and on-site monitoring data, the horizontal deformation of the enclosure structure is an important physical quantity that can better reflect the stability of the tunnel pit and its surroundings. It is very important to realise the accurate prediction of the horizontal deformation of the tunnel pit enclosure structure (Li et al., 2015). Therefore, this paper obtains the simulation results of the deep horizontal deformation of the enclosure structure at the end of two excavation. The monitoring data of deep horizontal deformation under the two working

conditions were compared with the simulation results. The curves drawn are shown in Figures 8 and 9.

Table 3. Suggested Values of Soil Elastic Modulus from Ground Investigation Report

Soil layer number	Modulus of compression E_s, MPa	Ratio of E to E_s	Modulus of elastic E, MPa
①-2 Topsoil	5.70	4.00	22.80
③-1 Silty clay	7.92	4.00	31.68
③-2 Silty clay	6.68	4.00	26.72
③-3 Silty clay	11.37	4.00	45.48

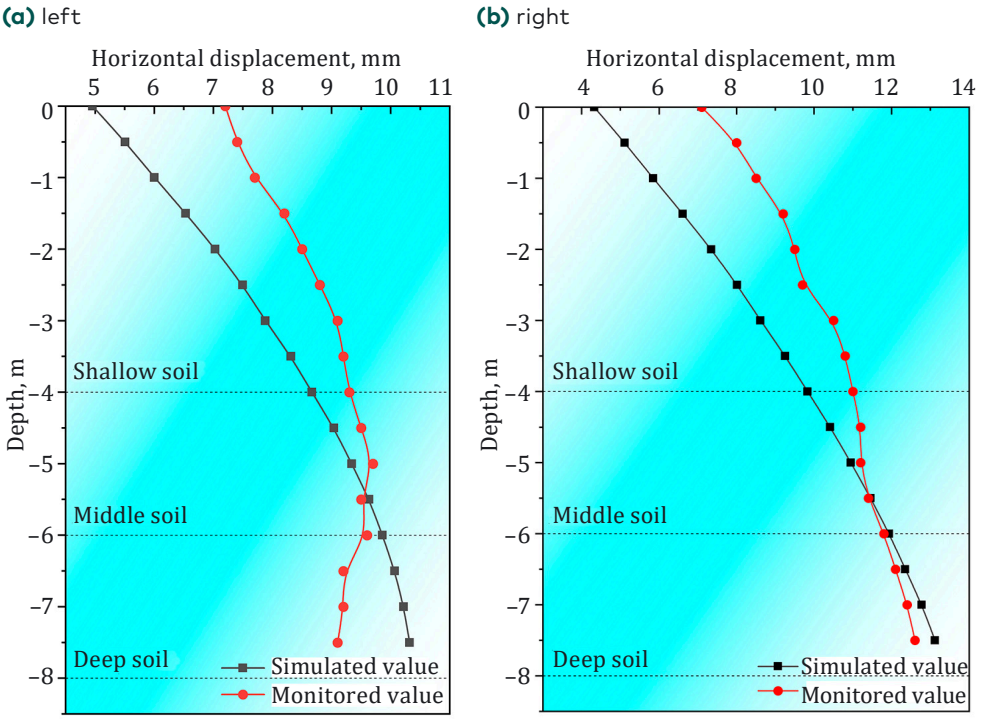

Figure 8. Comparison of deep horizontal deformation at the end of the second excavation

According to Figure 8, with the increase of the excavation, both the simulated and actual results of the deep horizontal deformation gradually increase. However, there are still great differences between the monitoring curve and the simulation

curve. Specifically, at the end of the second excavation, above −5.5 m, the simulated values of horizontal deformation of the enclosure structure are smaller than the actual values. The largest error is located at the surface, with an absolute error of 2.24 mm. The relative error reaches 31.20%. Below −5.5 m, the simulated values are larger than the actual values. At the depth of −7.5 m, the monitoring data is 8.6 mm, and the simulated data is 10.32 mm, with the relative error of 20.00%. While at the end of the third excavation, the relative error between simulated and actual values reaches 39.06% in the part above −5.5 m. The part below −5.5 m is better fitted, and the maximum relative error is only 4.11%.

Comparing the simulation results after the second and third excavations with the measured data, it is found that although the simulation results can predict the trend of the horizontal deformation under each excavation condition, there is a large deviation between the simulation results and the monitored value. This is mainly due to the fact that the physical parameters of the soil layer are not constant during the excavation process of the tunnel pit. It will change with excavation disturbance. As a result, the simulation results based on the ground investigation report cannot accurately express the real soil deformation at each excavation stage. Considering this factor, this paper adopted a more refined strategy. Using the compression modulus information, the variation range of elastic modulus of soil layer is reasonably defined. Then, the PSO and the SVM were combined to analyse the elastic modulus of soil layer. The inverted elastic modulus can be more suitable for soil characteristic changes in actual construction process. It provides more accurate parameters for the stability analysis and design optimisation of tunnel pit engineering.

2.2. Inversion analysis process and results

2.2.1. Training sample construction

Based on the literature (Li et al., 2017) and engineering experience, the ranges of the elastic modulus of the four soil layers were set as follows: The elastic modulus of the ①-2 layer soil (E_1): 5~9 MPa; the elastic modulus of the ③-1 layer soil (E_2): 6.5~10.5 MPa; the elastic modulus of the ③-2 layer soil (E_3): 15~31 MPa; and the elastic modulus of the ③-3 layer soil (E_4): 50~74 MPa. The range of elastic modulus was divided into five levels. The orthogonal experiment with 4 factors and 5 levels was designed. Thus, we obtained 25 orthogonal test combinations of elastic modulus. Each set of elastic modulus was substituted into the tunnel pit model for simulation. The deep horizontal deformation of the tunnel pit at the end of the second excavation was obtained. This calculation result was taken as the training sample of PSO-SVM, as shown in Table 4.

Table 4. Training samples obtained from orthogonal experimental design

Serial number	E_1, MPa	E_2, MPa	E_3, MPa	E_4, MPa	Horizontal deformation				
					1 m depth	3 m depth	5 m depth	6 m depth	7.5 m depth
1	5.00	6.50	15.00	50.00	9.670	10.768	11.504	11.699	11.607
2	5.00	7.50	19.00	56.00	8.572	9.618	10.320	10.506	10.426
3	5.00	8.50	23.00	62.00	7.753	8.740	9.400	9.573	9.490
4	5.00	9.50	27.00	68.00	7.116	8.042	8.657	8.814	8.722
5	5.00	10.50	31.00	74.00	6.608	7.474	8.043	8.184	8.079
6	6.00	6.50	19.00	62.00	8.679	9.508	10.022	10.121	9.890
7	6.00	7.50	23.00	68.00	7.844	8.649	9.151	9.250	9.041
8	6.00	8.50	27.00	74.00	7.193	7.964	8.443	8.538	8.338
9	6.00	9.50	31.00	50.00	6.653	8.180	9.322	9.732	10.098
10	6.00	10.50	15.00	56.00	8.836	9.894	10.597	10.774	10.653
11	7.00	6.50	23.00	74.00	7.939	8.579	8.938	8.972	8.650
12	7.00	7.50	27.00	50.00	7.321	8.750	9.802	10.164	10.432
13	7.00	8.50	31.00	56.00	6.768	8.059	8.996	9.310	9.507
14	7.00	9.50	15.00	62.00	8.911	9.758	10.277	10.369	10.100
15	7.00	10.50	19.00	68.00	8.079	9.240	10.041	10.273	10.272
16	8.00	6.50	27.00	56.00	7.440	8.628	9.469	9.733	9.828
17	8.00	7.50	31.00	62.00	6.867	7.959	8.723	8.955	9.010
18	8.00	8.50	15.00	68.00	8.992	9.650	10.006	10.023	9.625
19	8.00	9.50	19.00	74.00	8.074	8.740	9.113	9.146	8.801
20	8.00	10.50	23.00	50.00	7.475	8.929	9.993	10.356	10.604
21	9.00	6.50	31.00	68.00	6.962	7.878	8.489	8.651	8.582
22	9.00	7.50	15.00	74.00	9.074	9.563	9.773	9.723	11.973
23	9.00	8.50	19.00	50.00	8.359	9.680	10.621	10.918	11.031
24	9.00	9.50	23.00	56.00	7.573	8.788	9.644	9.908	9.985
25	9.00	10.50	27.00	62.00	6.965	8.084	8.864	9.098	9.139
Monitored value	–	–	–	–	6.900	8.800	9.800	9.500	8.600

2.2.2. Analysis of the results

Particle Swarm Optimisation was used to optimise the penalty parameters and Gaussian kernel function parameters of Support Vector Machine model. The values of the parameters in the PSO were as follows: We used the Linear decline strategy

as the inertial weight, and the value was reduced from 1.2 to 0.4. The number of particles was taken to be 30. The number of iterations was taken to be 300. The self-learning factor and the social-learning factor were all taken to be 2.0. The speed of the particles was taken to be 0.6. The range of penalty parameter in SVM was set from 0.1 to 1000. The range of kernel function parameter was set from 0.1 to 1000. The insensitivity parameter was taken to be 0.01. Running the program, the Particle Swarm Optimisation was used to search for the optimal model parameters. The optimal parameters were then put into the Support Vector Machine. The model was trained with normalized training samples. After the training completed, the actual monitoring data were input to obtain the inverse value of the elastic modulus. At the same time, the average fitness of particles with the number of iterations was obtained, as shown in Figure 9. Separately, the first type of particles reached the lowest fitness after 50 iterations. The third particle stabilised after nearly 300 iterations. The second and fourth particles reached the lowest fitness at about 200 times. Overall, after 300 iterations, the average fitness of the particles was stable, indicating that the PSO found the optimal solution.

Comparison of the inverse values of elastic modulus with the values of compressive modulus is provided in Table 5. The inverse values of elastic modulus of the four layers of soils were about 1, 1, 3, and 6 times of the compressive modulus.

Table 5. Comparison of the inversion values of elastic modulus and compression modulus of the soil layer

Ground level	Inverted elastic modulus E	Compression modulus E_s	E/E_s
①-2 layers of soil	6.95	5.70	1.22
③-1 layers of soil	8.12	7.92	1.02
③-2 layers of soil	20.56	6.68	3.07
③-3 layers of soil	67.42	11.37	5.92

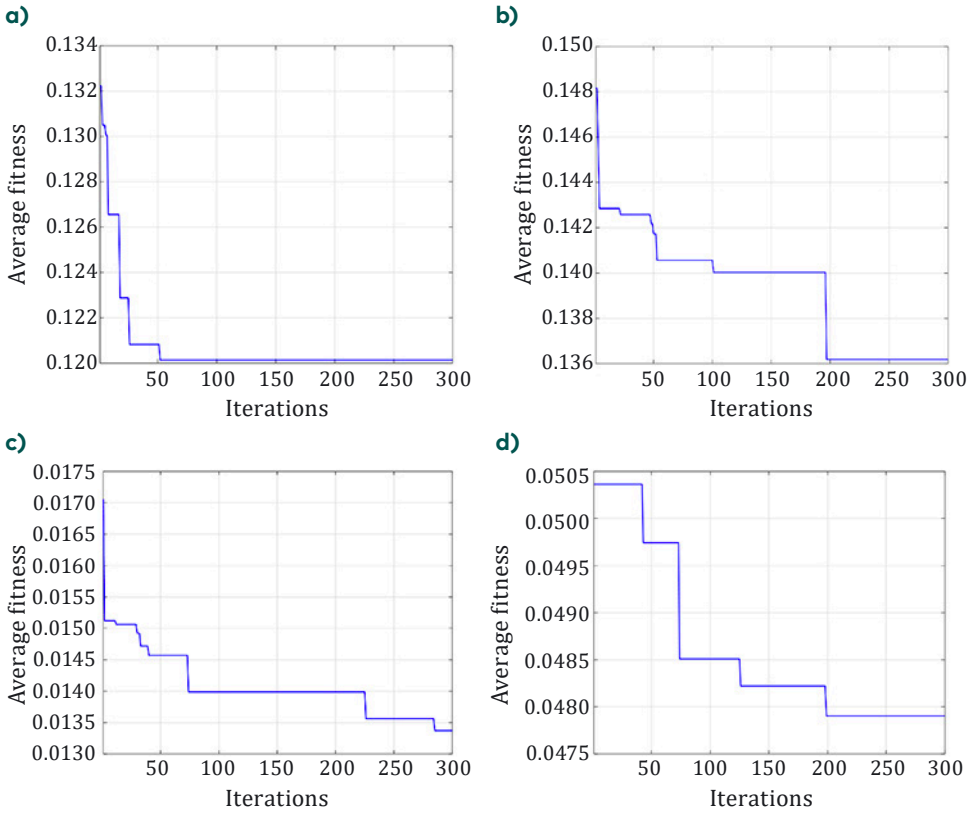

Figure 9. Curves of the average adaptation of the four particles with the number of iterations

After inputting the inversion value of elastic modulus into the finite element model, the horizontal deformation at different depths at the end of the second excavation was calculated. The deformation cloud diagrams are shown in Figure 10. The simulation results were compared with the monitored value (see Figure 11). It can be seen in Figure 11 that, if the inversion parameters were used for finite element simulation, the results would be consistent with the variation trend of the monitored value with depth. The maximum absolute error was 0.799 mm by comparing the finite element simulation results with the monitored value, and the maximum relative error was 11%. The average absolute error was 0.353 mm, and the mean relative error was 4.25%. Thus, the rationality and accuracy of the inversion method were verified.

It can also be seen from Figure 11 that the points with large differences between simulation and measurement were mainly concentrated in the shallow

soil layer. In contrast, the simulation results of middle and deep soil showed higher accuracy. In the face of this phenomenon, it was speculated that the shallow soil was more susceptible to various construction activities, such as mechanical equipment operations and traffic loads. However, middle and deep soils were less affected by such short-term disturbances. Overall, although there were some errors in the shallow range, the simulation results maintained a high consistency with the monitored value on the whole. Its accuracy could meet the engineering requirements.

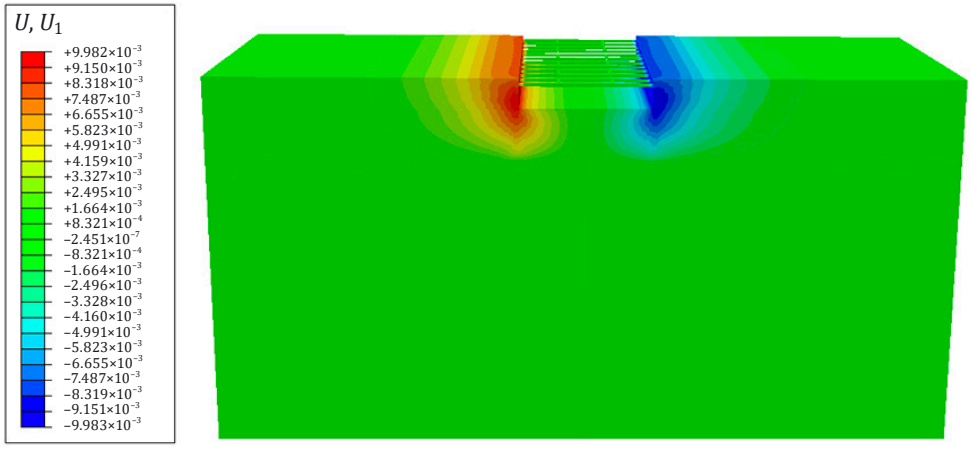

Figure 10. Cloud view of horizontal deformation of the pit at the end of the second excavation

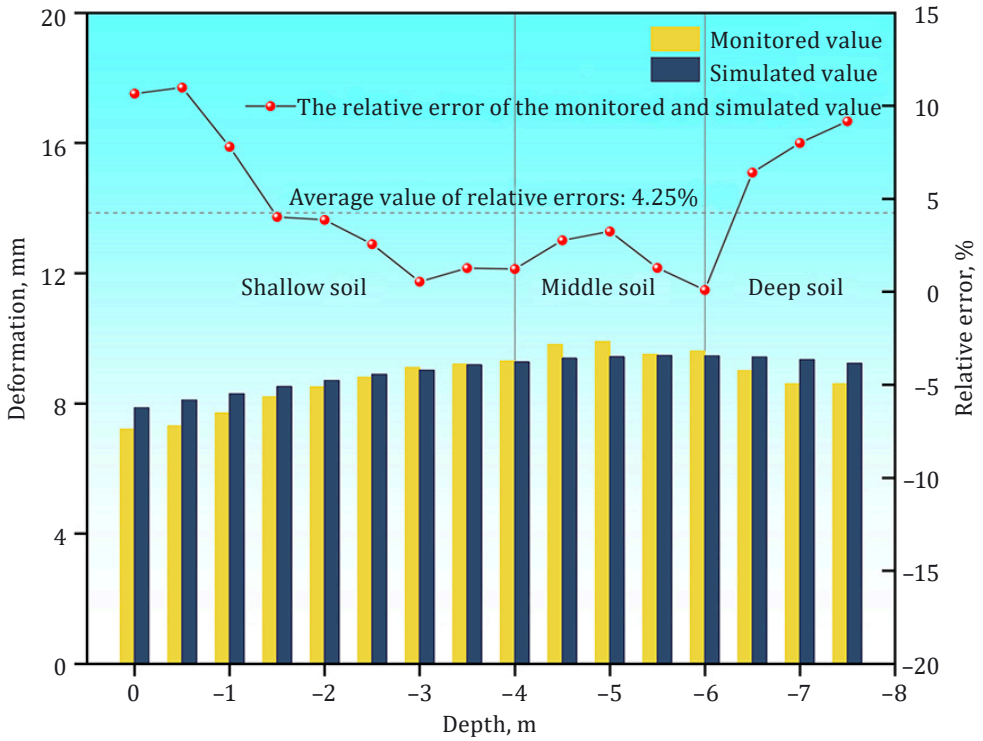

Figure 11. Comparison of the simulated and monitored values at the end of the second excavation

Based on the elastic modulus inversion result at the end of the second excavation, the simulation prediction of deep horizontal deformation at the end of the third excavation was carried out. The deformation cloud diagrams are shown in Figure 12. The comparison between the prediction result and the monitored value is shown in Figure 13. According to the prediction result, under the condition of unchanged enclosure structure, the maximum value of deep horizontal deformation at the end of the third excavation of the tunnel pit was about 12.6 mm. It was less than the monitoring warning value of 24 mm, so the construction was safe. Comparing the simulated results and monitored value, the maximum relative error was only 6.19%, and the average relative error was only 2.94%. It was shown that the simulated results were very close to the actual monitoring values.

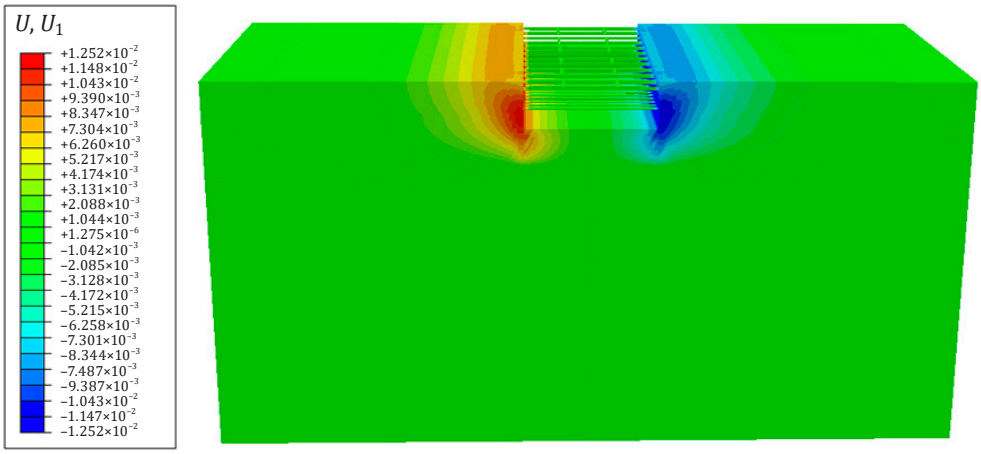

Figure 12. Cloud view of horizontal deformation of the pit at the end of the third excavation

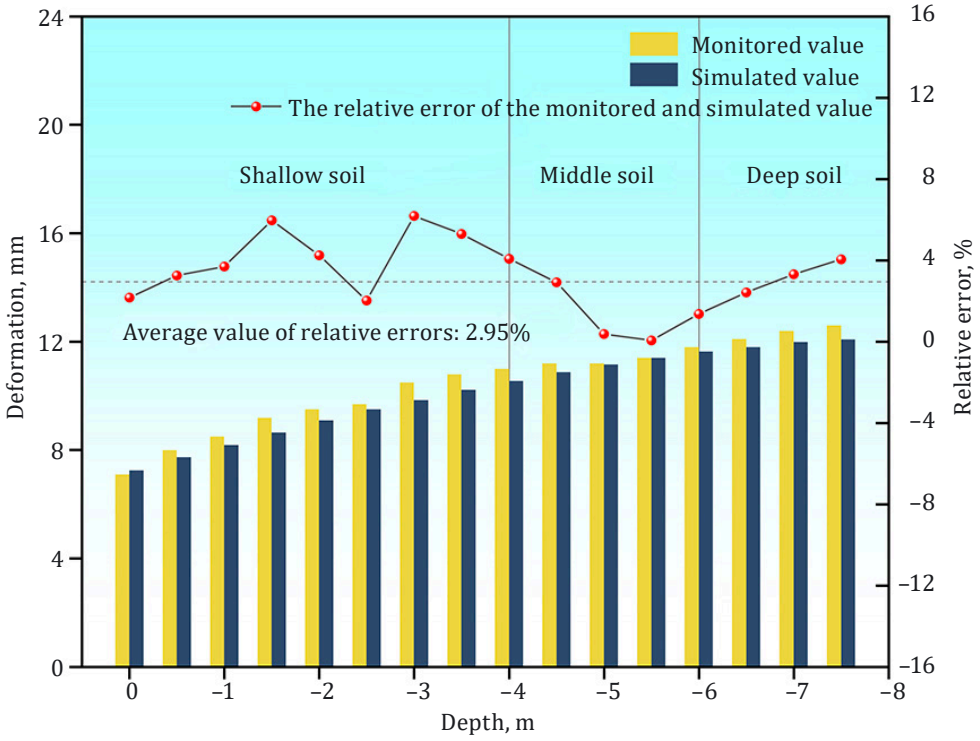

Figure 13. Comparison of the simulated and monitored values at the end of the third excavation

Conclusion

In this paper, taking Yilu Expressway Qingshan Tunnel Open-cut tunnel as an example, first, numerical simulation was carried out according to the ground investigation report. Then, according to the monitored value of the horizontal deformation, with the help of the SVM and the PSO, the elastic modulus of the four layers of soil at the end of the second excavation was inverted. Finally, the horizontal deformation of the enclosure structure at the end of the third excavation was predicted. The following conclusions were mainly obtained:

(1) The parameters provided in the ground investigation report were substituted into the finite element model for calculation; although the calculation results could express the trend of horizontal deformation, the simulation results differed greatly from the monitored value, which could not reach the accuracy of engineering application. Therefore, it was necessary to find more accurate parameters.

(2) The PSO-SVM was applied to the numerical simulation parameter inversion of tunnel pit. The method could make up for the deficiency of soil parameter error caused by disturbance in laboratory test. Then, a finite element model based on inverted parameters was established, which could accurately provide feedback on the real-time state of the pit construction enclosure structure.

(3) The inverted elastic modulus was substituted into the finite element model at the end of the second excavation to simulate the horizontal deformation. The average absolute error between the simulation results and the monitored value was 0.35 mm, and the average relative error was 4.25%. It showed that the inverted elastic modulus had the high accuracy, which verified the reasonableness of the method.

(4) Using the elastic modulus obtained from the inversion, the horizontal deformation for the next working condition was predicted. The calculation results had an average absolute error of 0.31 mm and an average relative error of 2.94% compared with the monitored value. The inversion parameters provided by this method could guide the engineering construction.

Acknowledgement

The authors wish to gratefully acknowledge the financial support from the Science and Technology Project of the Transport Engineering and Construction Bureau of Jiangsu Province.

Disclosure Statement

We do not have any competing financial, professional or personal interests with other parties.

REFERENCES

Amini, M., & Ardestani, A. (2019). Stability analysis of the North-Eastern slope of Daralou copper open pit mine against a secondary toppling failure. *Engineering Geology*, *249*, 89–101. https://doi.org/10.1016/j.enggeo.2018.12.022

Chen, B., Fu, X., Guo, Y.X., & Shao, C.F. (2015). Zoning elastic modulus inversion for high arch dams based on the PSOGSA-SVM method. *Advanced in Civil Engineering,* 145–156. https://doi.org/10.1155/2019/7936513

Cheng, Q.S., Yang Z.S., Qin S.W., Zhang, L., Miao, Q., & Zhang, Y. (2022). Application of soil parameters inversion based on PSO-MLSSVR in deep foundation pit engineering. *Journal of Engineering Geology*, *30*(2), 520–532. https://doi.org/10.13544/j.cnki.jeg.2021-0143

Feng, T.G., Wang, C.R., Zhang, J., Wang, B., & Jin Y.F. (2022). An improved artificial bee colony-random forest (IABC-RF) model for predicting the tunnel deformation due to an adjacent foundation pit excavation. *Underground Space*, *7*(4), 514–527. https://doi.org/10.1016/j.undsp.2021.11.004

Gao, D.F., Zhou, A., Feng, Y.T., et al. (2020). Deformation monitoring and back analysis of soil parameters in the cut and cover installation of Taihu tunnel. *Soil Engineering and Foundation*, *34*(3), 385–390.

Gioda, G, & Maier, G. (1981). Direct search solution of an inverse problem in elastoplasticity: identification angle and *in-situ* stress by pressure tunnel tests. *International Journal of Rock Mechanics and Mining Sciences and Geomechanics Abstracts*, *18*(2), 1823–1848. https://doi.org/10.1002/nme.1620151207

Guo, Q., Li, G.Q., Deng, C., Wu, J., Chen, Z.Y., & Xu, X.B. (2020). Rolling bearing fault diagnosis based on wavelet packet transform and convolutional neural network. *Applied Sciences*, 10(3), Article 770. https://doi.org/10.3390/app10030770

Jiang, A.N., Wang, S.Y., & Tang S.L. (2011). Feedback analysis of tunnel construction using a hybrid arithmetic based on Support Vector Machine and Particle Swarm Optimisation. *Automation in Construction*, *20*(4), 482–489. https://doi.org/10.1016/j.autcon.2010.11.016

Jiang, P. (2013). Back analysis method of foundation pit soil mechanical parameters based on GA-BP neural network. *Journal of Applied Sciences*, *13*(15), 3099–3103. https://doi.org/10.3923/jas.2013.3099.3103

Kavanagh, K.T., & Clough, R.W. (1971). Finite element applications in the characterization of elastic solids. *International Journal of Solids & Structures*, *7*(1), 11–23. https://doi.org/10.1016/0020-7683(71)90015-1

Kirsten, H.A.D. (1976). Determination of rock mass elastic moduli by back analysis of deformation measurement. *Proc. Symp. on Exploration for Rock Eng. Johannesburg*, 1154–1160.

Li, J., Zhou, S.C., Wang, L., et al. (2017). Methods for calculating the elastic modulus in numerical analysis of soft soil area. *China Water Transport*, *17*(5), 324–328.

Li, S., Yuan, Z.G., Wang, C., et al. (2018). Optimization of support vector machine parameters based on group intelligence algorithm. *CAAI Transactions on Intelligent Systems*, *13*(1), 70–84.

Li, Y.J., Xue, Y.D., Yue, L., & Chen B. (2015). Displacement prediction of deep foundation pit based on genetic algorithms and BP neural Network. *Chinese Journal of Underground Space and Engineering, 11*(S2), 741–749.

Li, B.Y., & Sima, J. (2021). Inverse analysis of horizontal displacement of foundation pit based on MEC-BP neural network. *J. Railw. Sci. Eng.*, *18*, 1764–1772. https://doi.org/10.19713/j.cnki.43-1423/u.t20210086

Li, H., Zhao, Z., & Du, X. (2022). Research and application of deformation prediction model for deep foundation pit based on LSTM. *Wireless Communications and Mobile Computing*, 463–478. https://doi.org/10.1155/2022/9407999

Li, Q., Cheng, F., & Zhang, X. (2024). Numerical simulation and deformation prediction of deep pit based on PSO-BP neural network inversion of soil parameters. *Sensors*, *24*(10), Article 2959. https://doi.org/10.3390/s24102959

Ling, T.H., Qin, J., Song, Q., & Hua, F. (2020). Intelligent displacement inverse analysis method based on improved particle swarm optimization and neural network and its application. *J. Railw. Sci. Eng.*, *17*, 2181–2190. https://doi.org/10.19713/j.cnki.43-1423/u.T20191119

Liu, H., Zhang, H.Q., & Liu, B. (2014). A prediction method for the deformation of excavations based on the particle Swarm optimization neural network. *Journal of Jilin University* (Earth Science Edition), *5*, 1609–1614. https://doi.org/10.13278/j.cnki.jjuese.201405204

Liu, Q., Yang, C.Y., & Lin, L. (2021). Deformation prediction of a deep foundation pit based on the combination model of wavelet transform and Gray BP neural network. *Mathematical Problems in Engineering*, 102–115. https://doi.org/10.1155/2021/2161254

Ma, H.H., Yuan, S., Zhang, Z., Tian, Y.H., & Dong, S.S. (2023). Application of soil parameter inversion method based on BP neural network in foundation pit deformation prediction. *Appl. Geophys.*, *20*, 299–309. https://doi.org/10.1007/s11770-023-1029-8

Ruan, Y.F., Gao, C.Q., Liu, K.W., et al. (2019). Inversion of rock and soil mechanics parameters based on particle swarm optimization wavelet support vector machine. *Rock and Soil Mechanics*, *40*(9), 3662–3669. https://doi.org/10.16285/j.rsm.2018.1055

Ruan, Y.F., Yu, D.X., Wu, L., et al. (2021). DE-GWO algorithm to optimize SVM inversion mechanical parameters of soft soil. *Chinese Journal of Geotechnical Engineering*, *43*(S1), 166–170.

Sha, Y.H., & Chen, Z.J. (2017). Application of PSO-SVM algorithm in soil parameters inversion. *Site Investigation Science and Technology*, *3*, 45–49.

Shen, Y.S., Wang, P., Li, M.P. & Mei, Q.W. (2019). Application of subway foundation pit engineering risk assessment: A case study of Qingdao rock area, China. *KSCE J. Civ. Eng.*, *23*(11), 4621–4630. https://doi.org/10.1007/s12205-019-1854-8

Wang, Z.L., Li, Y.C., & Shen, R.F. (2007). Correction of soil parameters in calculation of embankment settlement using a BP network back-analysis model. *Engineering Geology*, *91*(2–4), 168–177. https://doi.org/10.1016/j.enggeo.2007.01.007

Wang, Z.Y., Yang, Z.F., & Wang, S.J. (1998). A review on inverse analyses of displacements in rock mechanics. *Advances in Mechanics*, *28*(4), 488–498.

Xiao, M.Q., Liu, H., Peng, C.S., et al. (2017). Back analysis of deep soft soil parameters based on neural network. *Chinese Journal of Underground Space and Engineering*, *13*(1), 279–286.

Xu, Y., Zhao, Y., Jiang, Q., Sun, J., Tian, C., & Jiang, W. (2024). Machine-learning-based deformation prediction method for deep foundation-pit enclosure structure. *Applied Sciences*, *14*(3), Article 1273. https://doi.org/10.3390/app14031273

Yang, W., & Li, Q.Q. (2004). Survey on particle Swarm optimization algorithm. *Strategic Study of CAE*, *6*(5), 87–94.

Zhang, Z.H., Zhou, C.B., Xiao, Z., & Miao, G. (2013). Sensitivity analysis and orthogonal backward analysis of soil parameters for subway tunnel. *Journal of Central South University (Science and Technology)*, *44*(6), 2488–2493.

Zhao, J., Li, W., & Peng, Y. (2023). Analysis on intelligent deformation prediction of deep foundation pit with internal support based on optical fiber monitoring and HSS model. *Front. Mater.*, *10*, Article 1231303. https://doi.org/10.3389/fmats.2023.1231303

Zheng, G., Du, Y.M., Diao, Y.N., Deng, X., Zhu, G.P., & Zhang, L.M. (2016). Influenced zones for deformation of existing tunnels adjacent to excavations. *Chinese Journal of Geotechnical Engineering*. *38*(4), 599–612. https://doi.org/10.11779/CJGE201604003

Zhou, A., Wang, B., Li, J.T., Zhou, X., & Xia, W.J. (2022). Long-term stability analysis and deformation prediction of soft soil foundation pit in Taihu tunnel. *Journal of ZheJiang University (Engineering Science)*, *56*(4), 692–701.

Zhou, Y., Su, W. J., Ding, L.Y., Luo, H.B., & Peter, E.D.L. (2017). Predicting safety risks in deep foundation pits in subway infrastructure projects: Support Vector Machine approach. *Journal of Computing in Civil Engineering*, *31*(5), 292–300. https://doi.org/10.1061/(ASCE)CP.1943-5487.0000700